ORGANIC PROCESS RESEARCH & DEVELOPMENT
OPR&D

pubs.acs.org/OPRD

Article

Continuous Process Improvement in the Manufacture of Carfilzomib, Part 2: An Improved Process for Synthesis of the Epoxyketone Warhead

Matthew G. Beaver,* Xianqing Shi, Jan Riedel, Parth Patel, Alicia Zeng, Michael T. Corbett, Jo Anna Robinson, Andrew T. Parsons, Sheng Cui, Kyle Baucom, Michael A. Lovette, Elçin Içten, Derek B. Brown, Ayman Allian, Tawnya G. Flick, Wendy Chen, Ning Yang, and Shawn D. Walker

Cite This: https://dx.doi.org/10.1021/acs.oprd.0c00052

Read Online

ACCESS | Metrics & More | Article Recommendations | Supporting Information

ABSTRACT: The development and kilogram-scale demonstration of an improved process for the synthesis of the epoxyketone warhead of carfilzomib is described. Critical to the success of this process was: (1) development of a scalable asymmetric epoxidation protocol; (2) identification of a crystalline intermediate with improved physical properties for isolation; (3) discovery and optimization of epimerization conditions to set the target stereochemistry; and (4) introduction of a seeded-bed coaddition crystallization to facilitate isolation of the final low-melting target. The results of kilogram-scale demonstration runs are shared, including details of a continuous process for the safe execution of an exothermic Barbier-type Grignard process.

KEYWORDS: *asymmetric epoxidation, continuous manufacturing, carfilzomib*

INTRODUCTION

As described in the first part of this series (10.1021/acs.oprd.0c00051), efforts toward a detailed understanding of the commercial manufacture of epoxyketone **1** highlighted several opportunities for improvement in the life-cycle management phase of this program. Central to our approach was identification and development of a scalable asymmetric epoxidation method that could address challenges associated with the existing bleach epoxidation process and eliminate the requirement for column chromatography. Described herein are our efforts toward an improved route to (*S*,*R*)-epoxyketone **1**, an intermediate in the synthesis of carfilzomib (Figure 1).[1]

RESULTS AND DISCUSSION

Development of an Improved Synthesis of 1. The established oxidation procedure to prepare (*S*,*R*)-epoxyketone **1** employs a substrate-controlled bleach epoxidation to generate a mixture of epoxide diastereomers (ca. 2:1 dr) from enone **2** (Scheme 1). The poor stereoselectivity, coupled with the low melting point of the desired epoxyketone stereoisomer (41 °C), rendered crystallization of the product from the crude reaction stream impractical. A chromatographic purification step was required to reduce impurity content prior to the final isolation, resulting in a significant increase in solvent consumption, processing time, and analytical testing burden. Efforts to deliver an improved manufacturing process focused on the development of a stereoselective epoxidation strategy to minimize formation of the undesired diastereomer and facilitate crystallization of the target compound **1**.

Despite the breadth of literature precedent, rendering the epoxidation of olefin **2** asymmetric proved to be a significant challenge.[2] The electron-deficient nature of the substrate

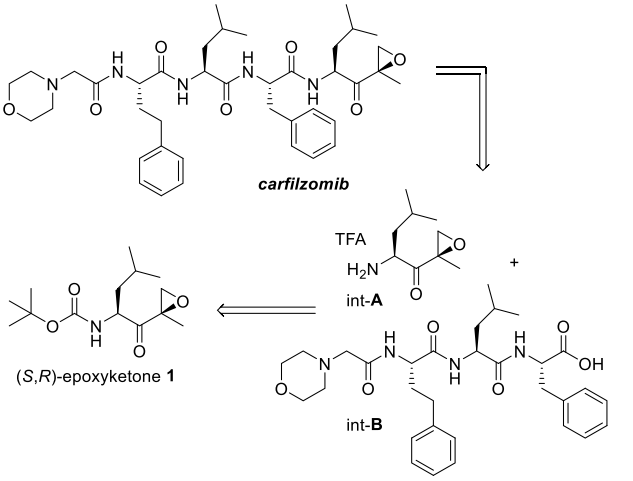

Figure 1. Epoxyketone intermediate in the synthesis of carfilzomib.

Scheme 1. Bleach Epoxidation to Synthesize Epoxyketone 1

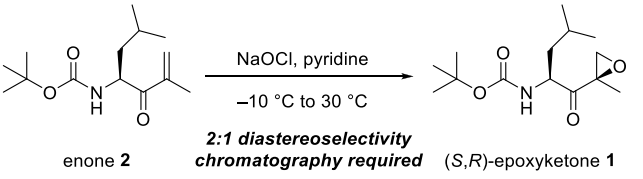

Received: February 10, 2020

https://dx.doi.org/10.1021/acs.oprd.0c00052
Org. Process Res. Dev. XXXX, XXX, XXX−XXX

necessitates a nucleophilic epoxidation method, which discounts many of the available asymmetric epoxidation methods. In addition, the substitution pattern adjacent to the ketone of olefin **2** challenges iminium ion and Lewis acid activation methods, which have proven to be useful approaches for the asymmetric epoxidation of α,β-unsaturated carbonyls.[3] Leveraging phase-transfer catalysis[4] resulted in poor conversions or epimerization of the labile amino-acid side chain. Approaches relying on redox manipulations of the ketone were evaluated but ultimately not selected due to the added synthetic steps and limited improvement to the overall control strategy.

Bioinspired nonheme manganese and iron complexes bearing tetradentate N-donor ligands have emerged as a class of bench-stable catalysts capable of oxidizing a wide range of olefins, including electron-deficient and sterically congested enones.[5] Of direct relevance to this effort, Sun and coworkers reported a manganese-catalyzed epoxidation protocol to prepare the target epoxyketone in high yield and good stereoselectivity, albeit with a preference for the undesired diastereomer.[6] The protocol utilizes a Mn-catalyst (**C1**) in the presence of H_2O_2 and acetic acid to prepare (*S*,*S*)-epoxyketone **3** in >95% assay yield for the combined epoxide stereoisomers and 88:12 dr, in excellent agreement with the literature report (Scheme 2). The enantiomer of enone **2** was then subjected to

Scheme 2. Mn-Catalyzed Asymmetric Epoxidation of Enone 2 by the Procedure of Sun and Coworkers

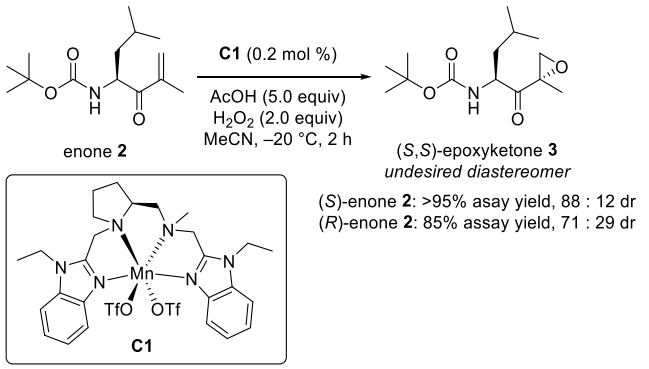

identical conditions to determine the influence of catalyst control on stereoselectivity. This experiment also delivered the undesired diastereomer as the major product but with decreased selectivity and yield, indicative of a mismatched catalyst−substrate combination (Scheme 2). These preliminary results encouraged further examination of the ligand architecture and reaction conditions to increase process efficiency.

Extensive evaluation of the reaction parameters, including ligand structure, metal and counterion, acid additive, oxidant, temperature, and solvent, were unsuccessful in identifying a system capable of overturning the apparent substrate-biased diastereoselectivity.[7] These optimization efforts culminated with the identification of an improved catalyst complex **C2** (Scheme 3) allowing for significantly decreased catalyst loading (0.04 mol %) while retaining high reaction yield (>95% assay yield) and diastereoselectivity (91:9 dr); however, the preference for the undesired (*S*,*S*)-epoxyketone **3** remained. The ligand can be prepared in a single step from commercially available materials. Complexation of the ligand

Scheme 3. Optimized Conditions for Oxidation of Enone 2

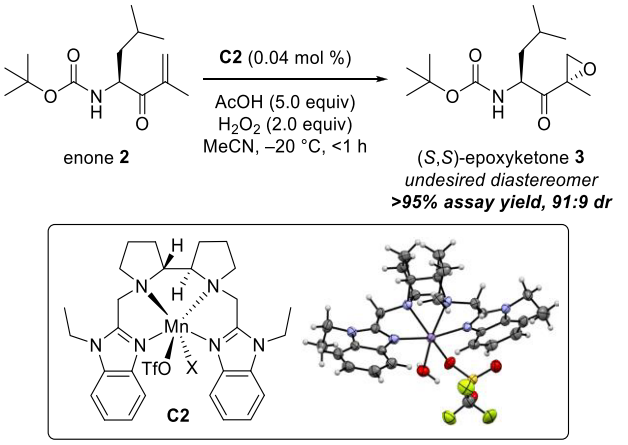

with $Mn(OTf)_2$ provided a crystalline and bench-stable catalyst complex.[8]

Despite an inability to overcome the substrate bias for formation of the undesired diastereomer, the solid-state phase behavior of (*S*,*S*)-epoxyketone **3** differed significantly from that of the target stereoisomer. Notably, the undesired diastereomer had an increased melting point (78 °C), rendering the compound amenable to a wider range of crystallization conditions and providing the opportunity to eliminate the use of chromatography in the synthetic route. The synthesis illustrated in Scheme 4 was proposed and served as the basis

Scheme 4. Proposed Route to Prepare (*S*,*R*)-Epoxyketone 1

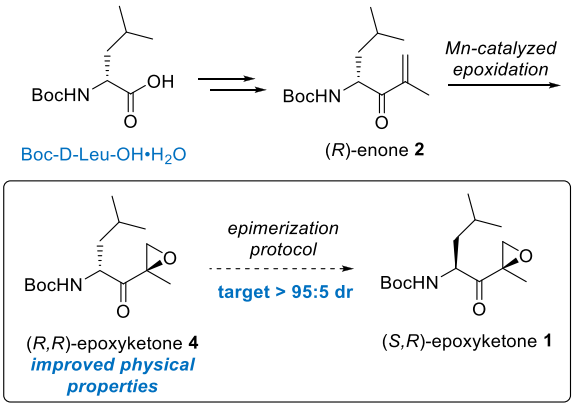

for further process development efforts, including: (1) preparation of (*R*)-enone **2** from unnatural Boc-D-leucine; (2) diastereoselective epoxidation and isolation by crystallization of (*R*,*R*)-epoxyketone **4** with high stereochemical purity; and (3) epimerization of the leucine side chain to prepare (*S*,*R*)-epoxyketone **1** with high stereoselectivity (target ≥95:5 dr) and purity, enabling a final isolation by crystallization of this low-melting compound.

As detailed in the previous manuscript of this series (10.1021/acs.oprd.0c00051), precedent existed for the stereochemical lability of the leucine side-chain of epoxyketone **1** in the presence of basic additives. Base identity impacted the selectivity of the epimerization and product stability, as summarized in Figure 2. Inorganic bases resulted in epimerization to form the desired stereoisomer but were associated with significant decomposition. A range of organic

https://dx.doi.org/10.1021/acs.oprd.0c00052
Org. Process Res. Dev. XXXX, XXX, XXX−XXX

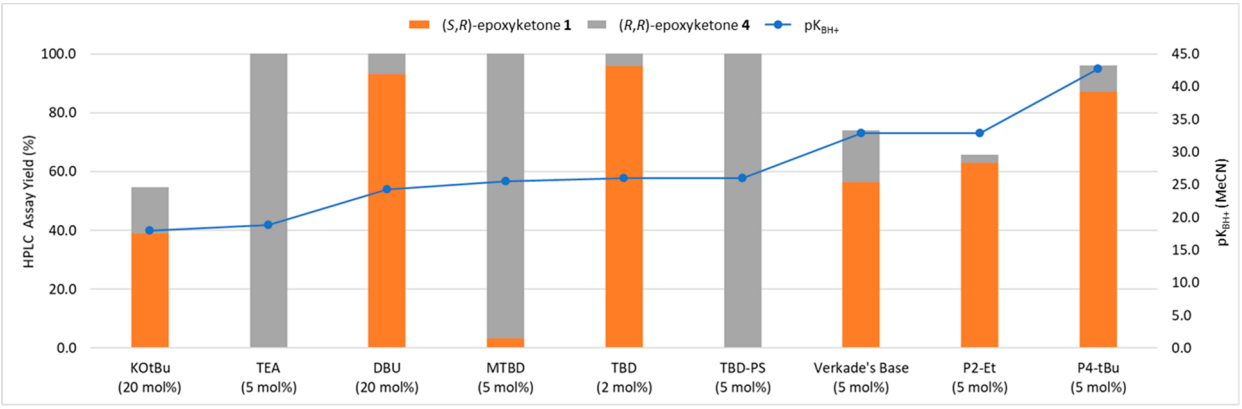

Figure 2. Effect of base on the epimerization and stability of (*R*,*R*)-epoxyketone **4**.

Scheme 5. Existing Route to Prepare Enone 2

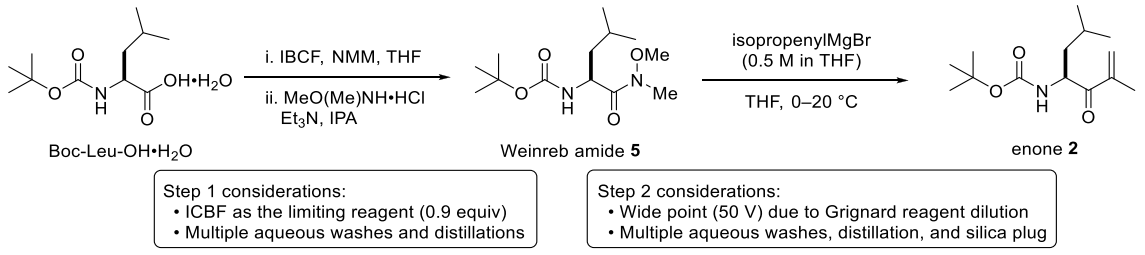

bases was investigated, demonstrating the requirement for a small, strong (i.e., pK_{BH+} > 20 as measured in acetonitrile),[9] non-nucleophilic base. Importantly, decomposition was suppressed, and a preference for the desired stereoisomer was observed, providing the requisite proof-of-concept required to advance this route. Use of triethylamine (TEA, pK_{BH+} = 18.8) did not result in formation of the desired isomer, even after extended aging at elevated temperatures. The use of 1,8-diazabicyclo[5.4.0]undec-7-ene (DBU, pK_{BH+} = 24.3) was productive in effecting the desired epimerization event while retaining near quantitative assay yields for the process. 1,5,7-Triazabicyclo[4.4.0]dec-5-ene (TBD, pK_{BH+} = 26.0) was similarly productive in generating the desired stereoisomer, whereas 7-methyl-triazabicyclo[4.4.0]dec-5-ene (MTBD, pK_{BH+} = 25.5) and polystyrene-bound TBD (pK_{BH+} = 26.0) were completely ineffective for this transformation, supporting the requirement for a nonhindered base. Sterically hindered phosphazene bases did not result in the desired epimerization, and use of less-hindered variants was accompanied by decomposition. Overall, a range of bases was found to be effective for this transformation, with diastereoselectivity governed by thermodynamic equilibrium and favoring the desired stereoisomer (ca. 95:5 dr at 20 °C). Importantly, the diastereoselectivity for epimerization met the required target purity to enable a final isolation by crystallization.

With lab-scale proof of concept established for the synthetic sequence illustrated in Scheme 4, efforts turned to the development of a robust, safe, and scalable solution for the manufacture of (*S*,*R*)-epoxyketone **1** from raw materials through final isolation in the absence of column chromatography.

Synthesis of (*R*)-Enone 2. The existing route to enone **2** is a two-step telescoped process from Boc-leucine−OH·monohydrate, as illustrated in Scheme 5. Development efforts for these steps focused on improving yield, purity profile, and throughput efficiency while retaining the overall bond-formation strategy.

Development efforts to prepare enone **2** initiated with optimization of the step 1 process, involving synthesis of Weinreb amide **5** via isobutylchloroformate-mediated amide-bond formation. The morpholine amide variant (**6**) was evaluated in preliminary experiments and found to perform comparably in both the coupling step and downstream processes; therefore, all subsequent studies focused on the preparation and use of this intermediate.[10] From the myriad of commercially available and well-precedented amide-bond forming reagents, *N*,*N*′-carbonyldiimidazole (CDI) provided the highest yield and purity profile in an initial evaluation to prepare morpholine amide **6**.[11] Formation of acyl imidazole intermediate **7** proceeded rapidly, as determined by *in situ* ReactIR measurements and corroborated by off-line UPLC analysis (Figure 3).[12] Of note, increasing the equivalence of CDI (from 1.2 to 2.0 equiv) enabled the direct use of Boc-Leu-OH·H_2O without drying via azeotropic distillation. Addition of morpholine to the reaction mixture resulted in rapid and complete consumption of intermediate **7** and generation of the desired morpholine amide **6**. A range of solvents were found to be effective for this transformation (e.g., 2-MeTHF, toluene, MTBE, THF, etc.); ultimately, 2-MeTHF was chosen for its ability to solubilize reaction byproducts (e.g., imidazole), effective partitioning through the aqueous wash sequence, and the ability to remove water via azeotropic distillation thus ensuring compatibility with the downstream process. Introduction of an aqueous HCl wash was sufficient to remove imidazole and excess morpholine from the organic stream, and an aqueous $NaHCO_3$ or Na_2CO_3 wash was effective in purging >5 mol % remaining starting material in the case of incomplete reaction conversion. Details of a representative kilogram-scale demonstration using MTBE as solvent to generate the desired morpholine amide **6** in 97% assay yield and >99.5 A% HPLC

https://dx.doi.org/10.1021/acs.oprd.0c00052
Org. Process Res. Dev. XXXX, XXX, XXX−XXX

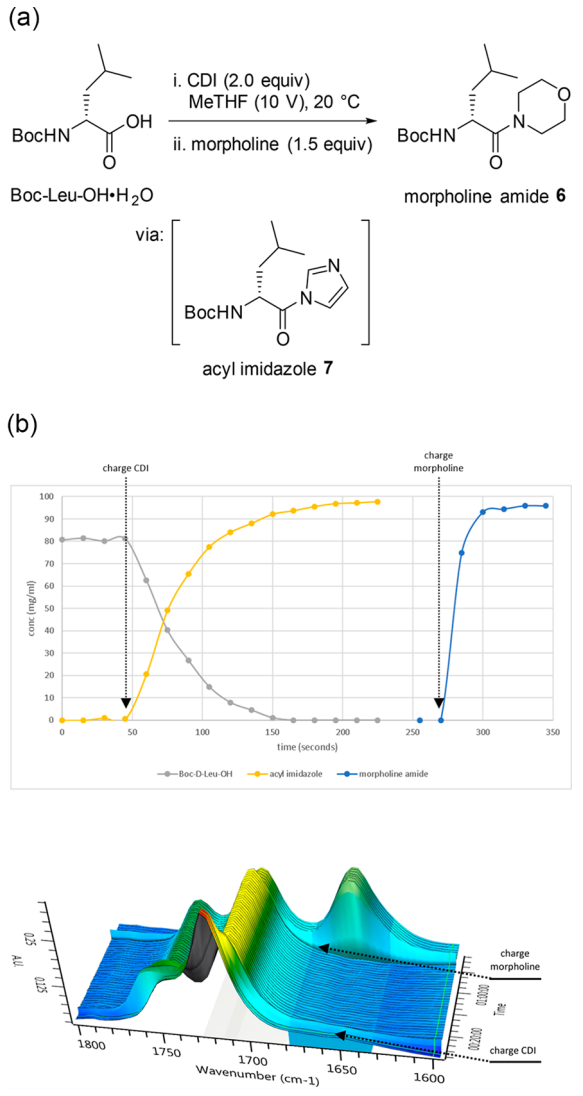

Figure 3. (a) Reaction progress as determined by quantitative *in situ* ReactIR measurements. (b) 3-D surface plot of IR spectra as a function of time and wavenumber.

achiral and chiral purity are available in the Experimental Section.

The step 2 process to prepare (*R*)-enone **2** involves addition of isopropenylmagnesium bromide to Weinreb amide **5** in THF (Scheme 5). The use of this commercially available Grignard reagent presents a significant bottleneck as its low solubility in THF (0.5 M) results in high dilution at the wide point of the existing batch process (50 volumes). The successful design, development, and implementation of a Barbier-type Grignard process avoids the cycle times associated with sourcing and titration of the preformed Grignard reagent and eliminates solubility considerations as the reagent is consumed on-demand.

Critical to both process safety and product quality for the Barbier process was control of the exothermic Grignard formation and a sequence of reactions including deprotonation (carbamate N−H) and nucleophilic addition to the carbonyl of morpholine amide **6**. Figure 4 illustrates the heat flow (W) associated with the portion-wise addition of 2-bromopropene to a reaction calorimeter containing magnesium turnings and morpholine amide **6** in THF/2-MeTHF at 40 °C. In the

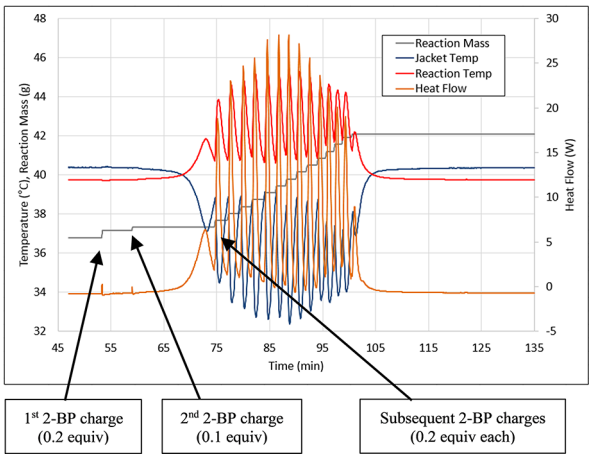

Figure 4. RC1 data for Barbier-type Grignard process to prepare enone **2**.

presence of a catalytic quantity of iodine, the initiation event typically occurs within 0.2−0.8 equiv of charged 2-bromopropene; in this specific experiment, the initiation proceeded upon addition and extended aging of 0.3 equiv 2-bromopropene. The total heat of reaction was calculated to be −1182 kJ/mol, corresponding to a 203 °C adiabatic temperature rise. ReactIR and UPLC methods were developed to monitor both the consumption of 2-bromopropene and the formation of product to mitigate the potential safety issues associated with accumulation of the Grignard precursor.

The high exothermicity of this process, together with variability observed for the initiation step, prompted development of a continuous process for the safe execution of this chemistry. Translation of the batch process to a continuous process utilizing continuously stirred tank reactors (CSTR) in series was accomplished with only minor changes to the procedure; for example, the THF/2-MeTHF ratio was optimized to facilitate improved solubility of the Grignard reagent to avoid clogging of the transfer lines or fouling of the magnesium turnings.[13] Proof-of-concept was completed at kg/day productivities utilizing a dual CSTR reaction platform followed by inline quench of the basic reaction medium with a 25 wt % citric acid solution and continuous phase separation. As depicted in Figure 5, a solution of morpholine amide **6** in THF/2-MeTHF was combined with 2-bromopropene (3.0 equiv) in CSTR1 (20 min, 40 °C) containing an excess of magnesium turnings.[14] The reaction solution was transferred from CSTR1 to CSTR2 (20 min, 40 °C) to achieve the required level of conversion (>95%) utilizing a peristaltic pump and particle-segregation tube to prevent transfer of solid magnesium turnings.[15,16] The crude reaction mixture from CSTR2 could then be combined with a 25 wt % citric acid solution and MTBE in CSTR3 to facilitate neutralization of the stream and phase separation, respectively. Through implementation of a continuous process, the reaction temperature of both reaction CSTRs could be controlled to within ±2.5 °C over the course of a 26 h demonstration, ensuring safe operation and delivery of kg-quantities of enone **2** in 89% yield with the requisite achiral (>90 A%) and chiral (>99.9 A%) purity profile for downstream processing.

The kilogram-scale demonstration of this process highlighted an additional safety benefit of continuous operation; that is, a single small-scale magnesium activation event was suitable to initiate Grignard formation and support the entirety

https://dx.doi.org/10.1021/acs.oprd.0c00052
Org. Process Res. Dev. XXXX, XXX, XXX−XXX

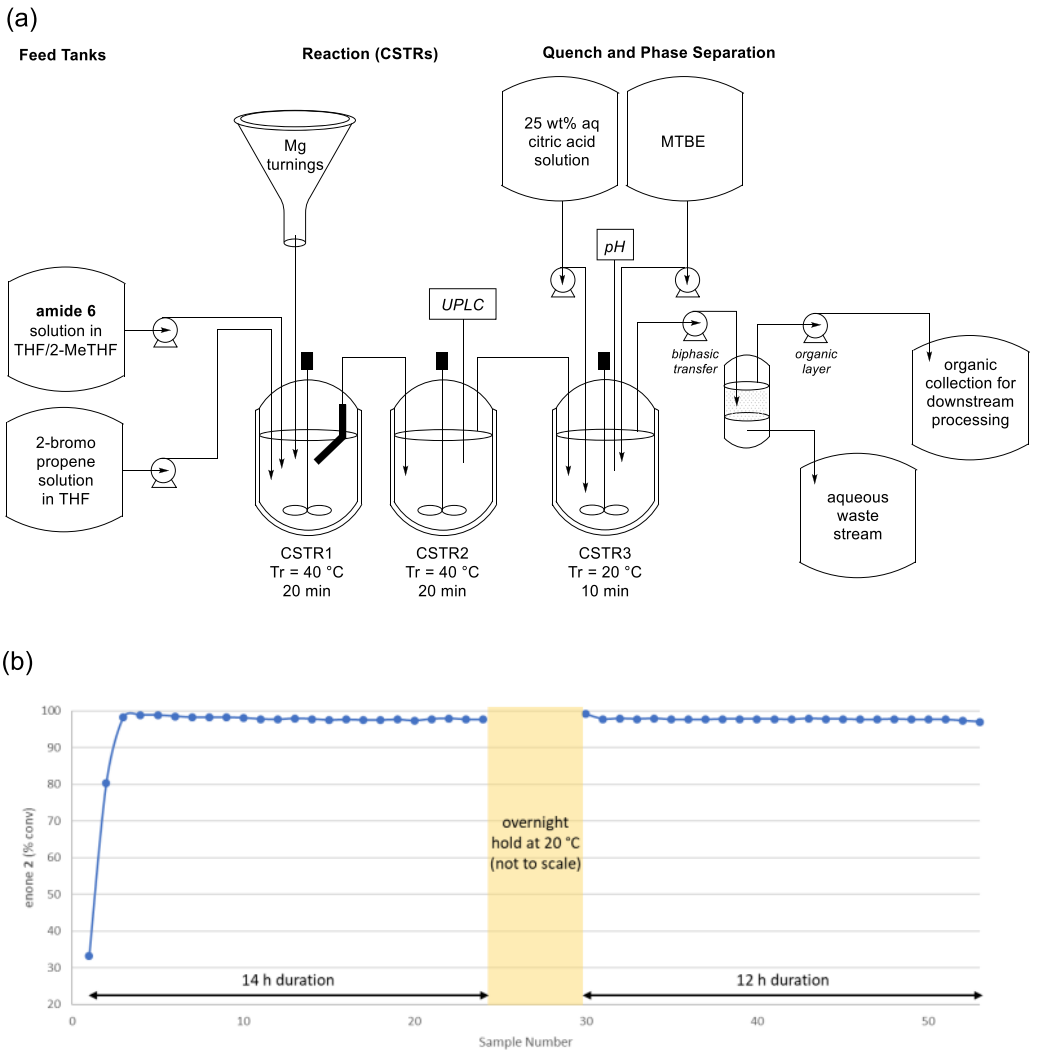

Figure 5. Details of the continuous process to prepare enone **2**. (a) Process flow diagram including reaction, inline quench, and phase separation. (b) Conversion values for enone **2** as determined by UPLC analysis of CSTR2.

of processing. For direct comparison, initiation of the multiday continuous process used 6.0 g of magnesium turnings, whereas the corresponding batch process would require a single charge of over 1 kg. Of the myriad magnesium activation options available,[17] prestirring the magnesium turnings with a catalytic quantity of iodine was demonstrated to provide a robust and well-controlled initiation process. Subsequent additions of 2-bromopropene resulted in immediate and reproducible exotherms (see Figure 4).

Synthesis of (*S,R*)-Epoxyketone 1. With an improved two-step telescoped process to deliver enone **2**, we next focused on the final steps to prepare the target (*S,R*)-epoxyketone **1**. The foundation for this two-step sequence, Mn-catalyzed epoxidation and epimerization, was established through the proof-of-concept efforts discussed in the previous section. Continued development was then required to optimize the reaction conditions, aqueous workup procedures, and intermediate and final isolations to achieve the target of eliminating column chromatography.

Reaction conditions for the Mn-catalyzed epoxidation to prepare epoxyketone **4** were established through the proof-of-concept studies (Scheme 3, *vide infra*). In summary, slow addition of a 50 wt % aqueous solution of H_2O_2 (2.0 equiv) to a cooled (−20 °C) solution of enone **2** and catalyst **C2** in ACN (10 volumes) and AcOH (5.0 equiv) generated the desired epoxide in >95% assay yield and a 91:9 mixture of diastereomers. Upon reaction completion, 5 volumes of a 25 wt % aqueous $NaHSO_3$ solution was charged to quench residual hydrogen peroxide and facilitate a phase separation. As illustrated in Table 1 below, the concentration and identity of the inorganic salt was critical for the efficient reduction of hydrogen peroxide, quality of phase cut with the water-miscible reaction milieu, and minimization of new impurities.

Critical to the success of this process was identification of conditions for isolation of this intermediate, (*R,R*)-epoxyketone **4**. A solubility screen identified several solvent systems capable of purging impurities generated in the telescoped upstream process. Among these options, crystallization from IPA/water was evaluated for ease of operation and demonstrated capacity to reject the undesired diastereomer generated from the epoxidation procedure. Solvent exchange from the reaction solvents to IPA could be performed with a single distillation to achieve ≤1.0 wt % ACN. The water content could then be adjusted to the target of 60 wt %, as informed by the IPA/water solubility profile (Figure 6) and capacity for rejection of the undesired epoxide diastereomer.

https://dx.doi.org/10.1021/acs.oprd.0c00052
Org. Process Res. Dev. XXXX, XXX, XXX−XXX

Table 1. Representative Survey of Aqueous Work-up Conditions

entry	conditions	comments	losses in aq phase (%)	peroxide test strip result
1	5 wt % $NaHSO_3$ (10 volumes)	no phase separation		positive
2	20 wt % $NaHSO_3$ (10 volumes)	clean phase cut	<1	negative
3	25 wt % $NaHSO_3$ (5 volumes)	clean and rapid phase separation	<1	negative
4	5 wt % Na_2SO_3 (10 volumes)	no phase separation		positive
5	20 wt % Na_2SO_3 (10 volumes)	precipitation of inorganic salts		negative
a	35 wt % Na_2SO_3 (3 volumes)	clean phase separation, new impurity at 2.2 A%	<1	negative

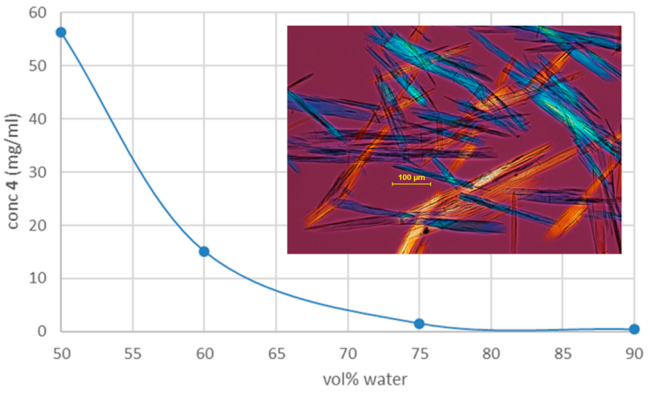

Figure 6. Solubility of epoxyketone **4** in IPA/water (20 °C) and representative polarized-light microscope image of isolated solids.

Cooling the batch to 5 °C served as an efficient strategy to minimize losses without impact to product quality. As designed, the epoxidation reaction, aqueous workup, and IPA/water crystallization could tolerate and reject process impurities generated in the preceding steps without the aid of column chromatography. Details of a representative kilogram-scale procedure to prepare (*R*,*R*)-epoxyketone **4** in 77% potency adjusted yield containing <0.5 A% epoxide diastereomer are available in the Experimental Section.

The high-purity crystalline solid isolated from step 3 could be subjected to the base-promoted epimerization procedure to generate a reaction solution of adequate purity to enable a final crystallization of the low-melting target compound **1**. Optimization of the epimerization process identified sub-stoichiometric quantities of DBU to be an effective promoter in a range of nonpolar organic solvents (e.g., MTBE, MeTHF, toluene, heptane, etc.). MTBE was selected due to the high solubility of both starting material and product, compatibility with aqueous workup, and facile exchange to the crystallization solvent (*vide infra*). Continued development of this process resulted in the procedure shown in Scheme 6. Addition of DBU (20 mol %) to a solution of (*R*,*R*)-epoxyketone **4** in 10 volumes MTBE results in a 95:5 dr favoring the target compound **1** after 10 h at 20 °C. A wash with 5 wt % aqueous $NaHSO_4$ served to remove DBU from the organic layer, and a final water wash purged residual inorganics. Representative material from this optimized process was used to support development of the final crystallization procedure to isolate

Scheme 6. Epimerization Process to Prepare Crude (*S*,*R*)-Epoxyketone 1

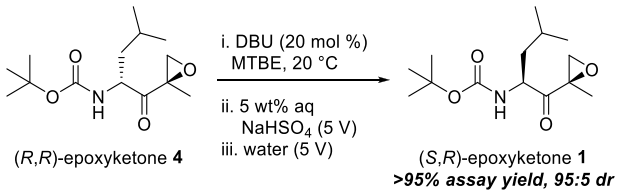

(*S*,*R*)-epoxyketone **1**, meeting targets for chiral and achiral purity.

The high solubility of epoxyketone **1** in a wide range of organic solvents prompted the use of water as antisolvent for isolation at reasonable processing temperatures. Unfortunately, an evaluation of aqueous-based solvent systems quickly identified a propensity for oiling (liquid–liquid phase separation). For example, addition of water to solutions of epoxyketone **1** in water-miscible cosolvents (e.g., NMP or MeOH) resulted in oiling and reactor fouling for a wide range of temperatures, solvent compositions, substrate concentrations, and addition rates. Attempts to determine solubility in a range of solvent systems highlighted increased temperature, vol % organic solvent, and epoxyketone **1** concentration as contributing to liquid–liquid phase separation (Figure 7). At

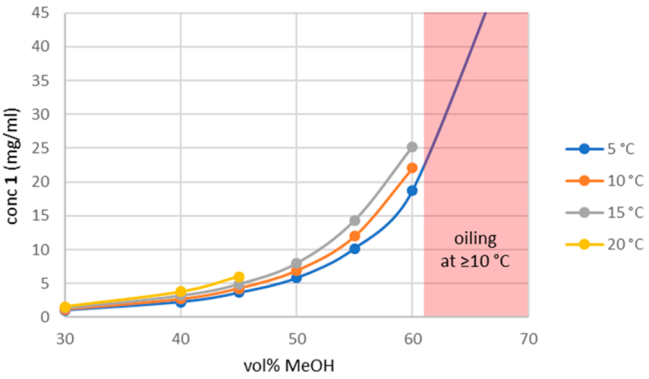

Figure 7. Solubility of epoxyketone **1** in MeOH/water as a function of solvent composition and temperature.

20 °C, equilibrating epoxyketone **1** in solvent compositions >45 vol % MeOH resulted in oils, whereas at 5 °C oils were not observed through 70 vol % MeOH. Based on these results and the requirement to purge 5 mol % diastereomer from the upstream process, a crystallization operating at an end-point of 50 vol % water at 5 °C was developed.

The solubility of epoxyketone **1** in MeOH/water and propensity for oil formation suggested the substrate should be isolated using a seeded batch coaddition process. This variety of process enables a constant solvent composition and supernatant concentration when addition rates are controlled to match desupersaturation kinetics. In this approach, two solutions (A) epoxyketone **1** in organic solvent and (B) water are added simultaneously and at the same rate to a preformed slurry of 5 wt % seed in 5 volumes 1:1 (v/v) MeOH/water at 5 °C (Figure 8). Water content and supernatant concentration can be monitored throughout the crystallization process and adjusted based on addition rates of the two streams. Keeping these values constant throughout the addition allows the execution of this process avoiding conditions where liquid–

https://dx.doi.org/10.1021/acs.oprd.0c00052
Org. Process Res. Dev. XXXX, XXX, XXX–XXX

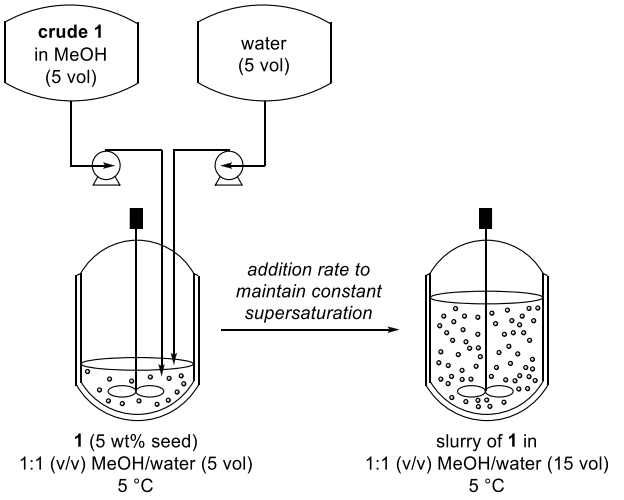

Figure 8. Illustration of the seeded batch coaddition crystallization procedure.

liquid phase separation occur, facilitating the isolation of this low-melting compound in a robust manner. Details of a representative kilogram-scale procedure to prepare (*S*,*R*)-epoxyketone **1** utilizing an analogous NMP/water seeded batch coaddition crystallization procedure are available in the Experimental Section.

CONCLUSIONS

An improved four-step process to prepare the epoxyketone warhead of carfilzomib was developed, which culminated in the elimination of column chromatography. The identification of a stereoselective epoxidation reaction, coupled with an understanding of the phase behavior of each stereoisomer, were critical to advance this approach. The process has been demonstrated on kilogram-scale to generate the target compound in over 50% yield with an E-factor reduction of 88% (2639 to 304).[18,19]

EXPERIMENTAL SECTION

General. All reactions were performed under an atmosphere of nitrogen under anhydrous conditions unless otherwise noted. All solvents and reagents were commercially obtained and used without further purification. ^{1}H NMR spectra were recorded at ambient temperature at 400 MHz using a Bruker AVANCE-400 spectrometer, and ^{13}C NMR spectra were recorded at 125 MHz using a Bruker AVANCE-500 spectrometer. The ^{1}H NMR data are reported as follows: chemical shift in parts per million (ppm) from an internal standard of residual $CHCl_3$ in $CDCl_3$ (7.27 ppm) on the δ scale, multiplicity (s = singlet, d = doublet, t = triplet, q = quartet, m = multiplet), coupling constants in hertz (Hz), and integration (H). Chemical shifts of ^{13}C NMR spectra are reported in ppm from the central peak of $CDCl_3$ (77.0 ppm). High resolution mass spectra (HRMS) were obtained using Agilent 1100 systems. Melting points were measured by differential scanning calorimetry (DSC) using a TA Instruments Q200 DSC at 10 °C/min.

Preparation of tert-Butyl (R)-(4-Methyl-1-morpholino-1-oxopentan-2-yl)carbamate ***6****.* A solution of (*tert*-butoxycarbonyl)-D-leucine·mohonohydrate (1.93 kg, 7.73 mol) in THF (4.8 L, 2.5 L/kg) was concentrated to 2 L/kg under vacuum while maintaining the temperature at <35 °C. Additional THF (4.8 L, 2.5 L/kg) was added, and the distillation was repeated. MTBE (9.6 L, 5.0 L/kg) was added; the solution was concentrated to 2 L/kg under vacuum while maintaining the temperature at <35 °C, and the resulting concentrate was reconstituted with MTBE (9.6 L, 5.0 L/kg). The solution was cooled to 0 °C, and a slurry of *N*,*N*′-carbonyldiimidazole (1.51 kg, 9.28 mol) in MTBE (7.7 L, 4.0 L/kg) was added over 25 min while maintaining the internal temperature at <5 °C. The reaction mixture was aged for an additional 1 h at 0 °C. To the cooled reaction mixture was added morpholine (1.01 kg, 11.6 mol) over 30 min while maintaining the internal temperature at <10 °C. The reaction mixture was aged for 1 h at 0 °C. A solution of 1 M aqueous HCl (6.8 L, 3.5 L/kg) was added, and the biphasic mixture was warmed to 20 °C. The layers were allowed to separate, and the bottom aqueous layer was removed. The organic layer was washed sequentially with 1 M aqueous HCl (2.9 L, 1.5 L/kg), 8 wt % aqueous $NaHCO_3$ (1.9 L, 1.0 L/kg), and 6 M aqueous NaCl (5.8 L, 3.0 L/kg) to afford an MTBE solution of morpholine amide **6** (2.25 kg, > 99.5 LCAP, 97% solution assay yield). A sample was characterized after concentration of the solution to provide the following analytical data: ^{1}H NMR (400 MHz, $CDCl_3$) δ 5.26 (d, J = 8.9 Hz, 1H), 4.62 (m, 1H), 3.45−3.72 (m, 8H), 1.71 (m, 1H), 1.42 (m, 11 H), 0.96 (d, J = 6.7 Hz, 3H), 0.92 (d, J = 6.5 Hz, 3H); ^{13}C NMR (125 MHz, $CDCl_3$) δ 171.6, 155.6, 79.6, 66.8, 66.6, 48.2, 46.0, 42.8, 42.4, 28.4, 24.6, 23.3, 22.0; HRMS (ESI-TOF) m/z calcd for $C_{15}H_{29}N_2O_4$ $(M + H)^+$ 301.2127, found 301.2126.

Preparation of tert-Butyl (R)-(2,6-Dimethyl-3-oxohept-1-en-4-yl)carbamate ***2****.* Two solutions were prepared for continuous addition to CSTR1: (A) a 0.658 M solution of morpholine amide **6** (5.22 kg, 17.4 mol) in 2.5:1 (v/v) THF/2-MeTHF (21.9 L, 4.20 L/kg) and (B) a 0.886 M solution of 2-bromopropene (6.61 kg, 51.9 mol) in THF (53.8 L, 10.3 L/kg).

Batch start-up of CSTR1 was performed to activate the magnesium turnings prior to continuous operation. To an inerted 1 L jacketed vessel (CSTR1) was charged magnesium turnings (6.04 g, 0.248 mol), a catalytic quantity of iodine, and morpholine amide solution A (0.120 L, 0.0776 mol). The reaction mixture was warmed to 40 °C, and 2-bromopropene (5.94 g, 0.0466 mol) was added in three equivalent portions and aged until initiation was confirmed by observation of an exothermic event and corroborated by *in situ* ReactIR. To the reaction mixture was added an additional quantity of 2-bromopropene (23.8 g, 0.186 mol) while maintaining the internal temperature at <45 °C.

A single bulk addition of magnesium turnings (59.2 g, 2.44 mol), corresponding to 12.0 equiv per CSTR turnover, was charged to CSTR1, and then continuous operation was commenced. To CSTR1 was pumped simultaneously feed solution A (15.4 mL/min, 10.1 mmol/min) and feed solution B (35.0 mL/min, 31.0 mmol/min). Both CSTR1 and CSTR2 were 1 L jacketed reactors with mean residence times of 20 min each, as dictated by the level of transfer tube. The internal reaction temperature was controlled at 40 °C, and the vessels were swept with nitrogen. A tube-in-tube transfer line was used between CSTR1 and CSTR2 to prevent solid magnesium transfer.[15] Additional magnesium turnings were charged in bulk portions at regular intervals to maintain 6−18 equiv magnesium with respect to morpholine amide **6** (per CSTR turnover).

https://dx.doi.org/10.1021/acs.oprd.0c00052
Org. Process Res. Dev. XXXX, XXX, XXX−XXX

The product stream from CSTR2 was transferred continuously to CSTR3 and combined with 25 wt % aqueous citric acid (28 mL/min, 9.0 L/kg) and MTBE (15 mL/min, 5.0 L/kg). CSTR3 was a 1 L glass-lined jacketed reactor with internal reaction temperature controlled at 20 °C and mean residence time of 5 min. The rapidly agitated biphasic mixture from CSTR3 was transferred to a settling vessel where the aqueous solution was diverted to waste and the organic layer was transferred to a collection vessel to afford a solution of enone **2** (3.64 kg, 94.4 LCAP, 89% solution assay yield) over 26 h of continuous operation. A sample was characterized after concentration of the solution to provide the following analytical data: ^{1}H NMR (400 MHz, $CDCl_3$) δ 6.09 (s, 1H), 5.89 (s, 1H), 5.10 (m, 2H), 1.91 (s, 3H), 1.74 (m, 1H), 1.49 (m, 1H), 1.44 (s, 9H), 1.34 (m, 1H), 1.01 (d, J = 6.5 Hz, 3H), 0.92 (d, J = 6.6 Hz, 3H); ^{13}C NMR (125 MHz, $CDCl_3$) δ 155.5, 142.4, 126.0, 105.0, 79.6, 52.6, 43.2, 28.4, 25.0, 23.4, 21.8, 17.8; HRMS (ESI-TOF) m/z calcd for $C_{14}H_{25}NNaO_3$ $(M + Na)^+$ 278.1732, found 278.1731.

A total of 75 kg of organic solution from continuous operation was subjected to batch workup and distillation. Aqueous wash of the product solution was performed in two identical batches: the organic solution was washed sequentially with 5 wt % aqueous NaCl (10 L, 4.0 L/kg), 8 wt % aqueous $NaHCO_3$ (13 L, 5.0 L/kg), and 5 wt % aqueous NaCl (10 L, 4.0 L/kg). The resulting organic solutions were combined and then concentrated to 2 L/kg under vacuum while maintaining the temperature at <30 °C. Acetonitrile (24 L, 5.0 L/kg) was added, and the solution concentrated to 2 L/kg under vacuum while maintaining temperature at <30 °C. The potency of the organic solution was then adjusted with acetonitrile in preparation for the downstream process.

Preparation of tert-Butyl ((R)-4-Methyl-1-((R)-2-methyloxiran-2-yl)-1-oxopentan-2-yl)carbamate ***4***. To a reactor containing a solution of enone **2** (1.09 kg, 4.28 mol) in acetonitrile (12 L, 11 L/kg) was charged catalyst **C2** (0.00139 kg, 0.00171 mol) and acetic acid (1.29 kg, 21.4 mol). The solution was cooled to −20 °C; a solution of 50 wt % aqueous hydrogen peroxide (0.583 kg, 8.57 mol) was added over 1.5 h while maintaining temperature at <−15 °C, and the reaction mixture was aged for 2 h at −20 °C. Upon reaction completion, the solution was warmed to 0 °C, and 35 wt % aqueous $Na_2S_2O_3$ (5.1 L, 4.7 L/kg) was added over 20 min while maintaining the temperature at <10 °C. The biphasic mixture was warmed to 20 °C; the layers were allowed to separate, and the bottom aqueous layer was removed. The organic layer was concentrated to 3 L/kg under vacuum while maintaining the temperature at <35 °C. Isopropanol (12 L, 11 L/kg) was added, and the solution was concentrated to 5 L/kg under vacuum while maintaining the temperature at <35 °C. Water (5.6 L, 5.1 L/kg) was added over 1.5 h, and the resulting slurry was cooled to 0 °C over 4 h. The slurry was then filtered, and the wet cake was washed twice with a cooled (0 °C) solution of 2:3 (v/v) isopropanol/water (2.4 L, 2.2 L/kg) and dried at 20 °C under vacuum to afford (R,R)-epoxyketone **4** (0.91 kg, 95.9 LCAP, 97.2 wt %, 77% yield) as a white crystalline solid: ^{1}H NMR (400 MHz, $CDCl_3$) δ 4.88 (m, 1H), 4.58 (m, 1H), 3.04 (d, J = 5.1 Hz, 1H), 2.86 (d, J = 5.1 Hz, 1H), 1.71 (m, 1H), 1.56 (s, 3H), 1.44 (s, 9H), 1.36 (m, 2H), 0.98 (d, J = 6.4 Hz, 3H), 0.93 (d, J = 6.6 Hz, 3H); ^{13}C NMR (125 MHz, $CDCl_3$) δ 207.8, 155.2, 79.8, 58.7, 52.9, 52.8, 41.1, 28.3, 24.9, 23.3, 21.5, 17.6; melting point = 77−78 °C; HRMS (ESI-TOF) m/z calcd for $C_{14}H_{25}NNaO_4$ $(M + Na)^+$ 294.1681, found 294.1680.

Preparation of tert-Butyl ((S)-4-Methyl-1-((R)-2-methyloxiran-2-yl)-1-oxopentan-2-yl)carbamate ***1***. To a 20 °C solution of (*R*,*R*)-epoxyketone **4** (1.03 kg, 3.79 mol) in MTBE (10 L, 10 L/kg) was charged 1,8-diazabicyclo[5.4.0]-undec-7-ene (0.116 kg, 0.762 mol) in a single portion. The reaction mixture was aged for 24 h at 20 °C, and a solution of 5 wt % aqueous $NaHSO_4$ (4.6 L, 4.5 L/kg) was added. The layers were allowed to separate, and the bottom aqueous layer was removed. The organic layer was washed with water (5.5 L, 5.4 L/kg) and then polish filtered to remove particulate matter. The solution was concentrated to 3 L/kg under vacuum while maintaining the temperature at <35 °C. NMP (2.1 L, 2.0 L/kg) was added, and the solution was concentrated under vacuum while maintaining temperature at <35 °C until a target of <1 wt % MTBE remained (ca. 3 L/kg). The solution was diluted with additional NMP (3.1 L, 3.0 L/kg) and transferred to a holding vessel. Simultaneous addition of the organic solution and an equal volume of water (6.1 L, 5.9 L/kg) to a precooled (5 °C) seed slurry of (*S*,*R*)-epoxyketone **1** (0.0515 kg, 0.200 mol) in 1:1 (v/v) NMP/water (5.1 L, 5.0 L/kg) proceeded over 9 h. The resulting slurry was then filtered, and the wet cake was washed twice with a cooled (5 °C) solution of 1:1 (v/v) NMP/water (2.1 L, 2.0 L/kg), twice with cooled (5 °C) water (2.1 L, 2.0 L/kg), and dried at 20 °C under vacuum to afford (S,*R*)-epoxyketone **1** (0.89 kg, 98.6 LCAP, 97.4 wt %, 79% yield) as a white crystalline solid: ^{1}H NMR (400 MHz, $CDCl_3$) δ 4.86 (d, J = 8.5 Hz, 1H), 4.31 (m, 1H), 3.29 (d, J = 4.9 Hz, 1H), 2.88 (d, J = 5.0 Hz, 1H), 1.72 (m, 1H), 1.51 (s, 3H), 1.48 (m, 1H), 1.41 (s, 9H), 1.17 (m, 1H), 0.96 (d, J = 6.5 Hz, 3H), 0.93 (d, J = 6.6 Hz, 3H); ^{13}C NMR (125 MHz, $CDCl_3$) δ 209.5, 155.6, 79.7, 59.0, 52.3, 51.4, 40.5, 28.3, 25.1, 23.4, 21.3, 16.8; melting point = 39−41 °C; HRMS (ESI-TOF) m/z calcd for $C_{14}H_{25}NNaO_4$ $(M + Na)^+$ 294.1681, found 294.1681.

■ ASSOCIATED CONTENT

Supporting Information

The Supporting Information is available free of charge at https://pubs.acs.org/doi/10.1021/acs.oprd.0c00052.

Additional experimental details (PDF)

C2 crystallographic information file (CIF)

■ AUTHOR INFORMATION

Corresponding Author

Matthew G. Beaver − *Process Development, Amgen, Inc., Cambridge, Massachusetts 02142, United States;* orcid.org/0000-0003-3816-4601; Email: mbeaver@amgen.com

Authors

Xianqing Shi − *Process Development, Amgen, Inc., Thousand Oaks, California 91320, United States*

Jan Riedel − *Process Development, Amgen, Inc., Cambridge, Massachusetts 02142, United States*

Parth Patel − *Process Development, Amgen, Inc., Cambridge, Massachusetts 02142, United States*

Alicia Zeng − *Process Development, Amgen, Inc., Cambridge, Massachusetts 02142, United States*

Michael T. Corbett − *Process Development, Amgen, Inc., Thousand Oaks, California 91320, United States*

https://dx.doi.org/10.1021/acs.oprd.0c00052
Org. Process Res. Dev. XXXX, XXX, XXX−XXX

Jo Anna Robinson − *Process Development, Amgen, Inc., Cambridge, Massachusetts 02142, United States*
Andrew T. Parsons − *Process Development, Amgen, Inc., Cambridge, Massachusetts 02142, United States;* orcid.org/0000-0002-0320-0919
Sheng Cui − *Process Development, Amgen, Inc., Cambridge, Massachusetts 02142, United States*
Kyle Baucom − *Process Development, Amgen, Inc., Thousand Oaks, California 91320, United States*
Michael A. Lovette − *Process Development, Amgen, Inc., Thousand Oaks, California 91320, United States*
Elçin Içten − *Process Development, Amgen, Inc., Cambridge, Massachusetts 02142, United States*
Derek B. Brown − *Process Development, Amgen, Inc., Thousand Oaks, California 91320, United States;* orcid.org/0000-0002-7909-0867
Ayman Allian − *Process Development, Amgen, Inc., Thousand Oaks, California 91320, United States*
Tawnya G. Flick − *Process Development, Amgen, Inc., Thousand Oaks, California 91320, United States;* orcid.org/0000-0001-7266-8999
Wendy Chen − *Process Development, Amgen, Inc., Thousand Oaks, California 91320, United States*
Ning Yang − *Process Development, Amgen, Inc., Cambridge, Massachusetts 02142, United States*
Shawn D. Walker − *Process Development, Amgen, Inc., Cambridge, Massachusetts 02142, United States*

Complete contact information is available at: https://pubs.acs.org/10.1021/acs.oprd.0c00052

Notes

The authors declare no competing financial interest.

■ ACKNOWLEDGMENTS

We thank Yasmin Alaee, Jiemin Bao, and Guilong Cheng for analytical contributions. We thank Kumar Ranganathan, Simone Spada, and John Huckins for their contributions to develop and demonstrate the process. We thank Richard Staples for performing the included single crystal X-ray analysis.

■ REFERENCES

(1) Siegel, D. S.; Martin, T.; Wang, M.; Vij, R.; Jakubowiak, A. J.; Lonial, S.; Trudel, S.; Kukreti, V.; Bahlis, N.; Alsina, M.; Chanan-Khan, A.; Buadi, F.; Reu, F. J.; Somlo, G.; Zonder, J.; Song, K.; Stewart, A. K.; Stadtmauer, E.; Kunkel, L.; Wear, S.; Wong, A. F.; Orlowski, R. Z.; Jagannath, S. A phase 2 study of single-agent carfilzomib (PX-171−003-A1) in patients with relapsed and refractory multiple myeloma. *Blood* **2012**, *120*, 2817−2825.

(2) For select reviews, see: (a) Xia, Q.-H.; Ge, H.-Q.; Ye, C.-P.; Liu, Z.-M.; Su, K.-X. Advances in Homogeneous and Heterogeneous Catalytic Asymmetric Epoxidation. *Chem. Rev.* **2005**, *105*, 1603−1662. (b) De Faveri, G.; Ilyashenko, G.; Watkinson, M. Recent advances in catalytic asymmetric epoxidation using the environmentally benign oxidant hydrogen peroxide and its derivatives. *Chem. Soc. Rev.* **2011**, *40*, 1722−1760. (c) Zhu, Y.; Wang, Q.; Cornwall, R. G.; Shi, Y. Organocatalytic Asymmetric Epoxidation and Aziridination of Olefins and Their Synthetic Applications. *Chem. Rev.* **2014**, *114*, 8199−8256. (d) Davis, R. L.; Stiller, J.; Naicker, T.; Jiang, H.; Jørgensen, K. A. Asymmetric organocatalytic epoxidations: reactions, scope, mechanisms, and applications. *Angew. Chem., Int. Ed.* **2014**, *53*, 7406−7426. (e) Bryliakov, K. P. Catalytic Asymmetric Oxygenations with the Environmentally Benign Oxidants H_2O_2 and O_2. *Chem. Rev.* **2017**, *117*, 11406−11459.

(3) See, for example: (a) Marigo, M.; Franzén, J.; Poulsen, T. B.; Zhuang, W.; Jørgensen, K. A. Asymmetric Organocatalytic Epoxidation of α,β-Unsaturated Aldehydes with Hydrogen Peroxide. *J. Am. Chem. Soc.* **2005**, *127*, 6964−6965. (b) Bondzic, B. P.; Urushima, T.; Ishikawa, H.; Hayashi, Y. Asymmetric Epoxidation of α-Substituted Acroleins Catalyzed by Diphenylprolinol Silyl Ether. *Org. Lett.* **2010**, *12*, 5434−5437. (c) Nemoto, T.; Ohshima, T.; Yamaguchi, K.; Shibasaki, M. Catalytic Asymmetric Epoxidation of Enones Using La−BINOL−Triphenylarsine Oxide Complex: Structural Determination of the Asymmetric Catalyst. *J. Am. Chem. Soc.* **2001**, *123*, 2725−2732. (d) Jacques, O.; Richards, S. J.; Jackson, R. F. W. Catalytic asymmetric epoxidation of aliphatic enones using tartrate-derived magnesium alkoxides. *Chem. Commun.* **2001**, 2712−2713.

(4) See, for example: (a) Corey, E. J.; Zhang, F. Y. Mechanism and Conditions for Highly Enantioselective Epoxidation of α,β-Enones Using Charge-Accelerated Catalysis by a Rigid Quaternary Ammonium Salt. *Org. Lett.* **1999**, *1*, 1287−1290. (b) Lifchits, O.; Mahlau, M.; Reisinger, C. M.; Lee, A.; Fares, C.; Polyak, I.; Gopakumar, G.; Thiel, W.; List, B. The Cinchona Primary Amine-Catalyzed Asymmetric Epoxidation and Hydroperoxidation of α,β-Unsaturated Carbonyl Compounds with Hydrogen Peroxide. *J. Am. Chem. Soc.* **2013**, *135*, 6677−6693.

(5) For select reviews, see: (a) Cussó, O.; Ribas, X.; Costas, M. Biologically inspired non-heme iron-catalysts for asymmetric epoxidation; design principles and perspectives. *Chem. Commun.* **2015**, *51*, 14285−14298. (b) Bryliakov, K. *Environmentally Sustainable Catalytic Asymmetric Epoxidations*; Taylor & Francis Group: New York, 2015.

(6) Wang, B.; Miao, C.; Wang, S.; Xia, C.; Sun, W. Manganese Catalysts with C_1-Symmetric N_4 Ligand for Enantioselective Epoxidation of Olefins. *Chem. - Eur. J.* **2012**, *18*, 6750−6753.

(7) A summary of the reaction parameters investigated is available in the Supporting Information

(8) Details of the synthesis are available in the Supporting Information. The observed displacement of a triflate anion in the single crystal X-ray structure likely occurred during the isolation from ACN/water. No negative impact was observed upon subjecting this catalyst to the epoxidation chemistry.

(9) Kaljurand, I.; Kütt, A.; Sooväli, L.; Rodima, T.; Mäemets, V.; Leito, I.; Koppel, I. A. Extension of the Self-Consistent Spectrophotometric Basicity Scale in Acetonitrile to a Full Span of 28 pKa Units: Unification of Different Basicity Scales. *J. Org. Chem.* **2005**, *70*, 1019−1028.

(10) For select examples of morpholine amides used in ketone synthesis, see: (a) Brown, J. D. Asymmetric synthesis of naproxen via a pinacol-type reaction. *Tetrahedron: Asymmetry* **1992**, *3*, 1551−1552. (b) Martin, R.; Romea, P.; Tey, C.; Urpi, F.; Vilarrasa, J. Simple and Efficient Preparation of Ketones from Morpholine Amides. *Synlett* **1997**, *12*, 1414−1416. (c) Sengupta, S.; Mondal, S.; Das, D. Amino acid derived morpholine amides for nucleophilic α-amino acylation reactions: A new synthetic route to enantiopure α-amino ketones. *Tetrahedron Lett.* **1999**, *40*, 4107−4110. (d) Jackson, M. M.; Leverett, C.; Toczko, J. F.; Roberts, J. C. An Unexpected Equilibrium Process Associated with a Standard Approach to Ynone Synthesis. *J. Org. Chem.* **2002**, *67*, 5032−5035.

(11) For a recent review, see: Dunetz, J. R.; Magano, J.; Weisenburger, G. A. Large-Scale Applications of Amide Coupling Reagents for the Synthesis of Pharmaceuticals. *Org. Process Res. Dev.* **2016**, *20*, 140−177.

(12) UPLC analysis was accomplished by derivatization of the acyl imidazole intermediate with a 10 wt % solution of morpholine in acetonitrile.

(13) Braden, T. M.; Johnson, M. D.; Kopach, M. E.; McClary Groh, J.; Spencer, R. D.; Lewis, J.; Heller, M. R.; Schafer, J. P.; Adler, J. J. Development of a Commercial Flow Barbier Process for a Pharmaceutical Intermediate. *Org. Process Res. Dev.* **2017**, *21*, 317−326.

(14) Details of the magnesium charge schedule are noted in the Experimental Section.

https://dx.doi.org/10.1021/acs.oprd.0c00052
Org. Process Res. Dev. XXXX, XXX, XXX−XXX

(15) Wong, S.-W.; Changi, S. M.; Shields, R.; Bell, W.; McGarvey, B.; Johnson, M. D.; Sun, W.-M.; Braden, T. M.; Kopach, M. E.; Spencer, R. D.; Flanagan, G.; Murray, M. Kinetics Model for Designing Grignard Reactions in Batch or Flow Operations. *Org. Process Res. Dev.* **2016**, *20*, 540−550.

(16) Reaction conversion in CSTR1 ranged from 90−95% upon achieving a state-of-control during continuous operation. Empirical evidence supported the inclusion of a second reactor to improve reaction conversion; a CSTR was chosen instead of a plug-flow reactor to minimize the risk of clogging if solid magnesium particles were transferred from CSTR1. Detailed computational modeling was performed to validate this approach and is the subject of a separate communication.

(17) Tilstam, U.; Weinmann, H. Activation of Mg Metal for Safe Formation of Grignard Reagents on Plant Scale. *Org. Process Res. Dev.* **2002**, *6*, 906−910.

(18) Environmental (*E*) factor = (kg of waste)/(kg of product). See: Sheldon, R. A. The E Factor: fifteen years on. *Green Chem.* **2007**, *9*, 1273−1283.

(19) Beaver, M.; Cui, S.; Xianqing, S.Synthesis of (*S*)-2-Amino-4-methyl-1-((*R*)-2-methyloxirane-2-yl)-pentan-1-one and Pharmaceutically Acceptable Salts Thereof. WO2018/027021A1, 2018.

https://dx.doi.org/10.1021/acs.oprd.0c00052
Org. Process Res. Dev. XXXX, XXX, XXX−XXX